

# Modeling the formation of cell-matrix adhesions in 3D matrices

J. Escribano<sup>a</sup>, M.T. Sánchez,<sup>b</sup> J.M. García-Aznar<sup>a,\*</sup>

<sup>a</sup>*Multiscale in mechanical and biological engineering (M2BE), University of Zaragoza, Zaragoza, Spain*

<sup>b</sup>*Centro Universitario de la Defensa Zaragoza Academia General Militar, Spain*

---

## Abstract

Cell migration is crucial in a wide variety of biological process like development, homeostasis or tissue regeneration. In particular, the interaction between the extracellular matrix and the cytoskeleton is a recurrent topic, due to its important role in this process. These interactions are built through protein clutches, generally known as focal adhesions or focal contacts. For migratory cells, these focal adhesions together with force generating processes in the cytoskeleton are responsible of the formation of protrusion structures like lamellipodia or filopodia, that determine the cell migration path. This phenomenon has been deeply studied in two-dimensional (2D) cases; however, the knowledge we have in the three-dimensional (3D) case is limited. In this work, we simulate different local extracellular matrix properties in order to unravel the fundamental mechanisms that regulate the formation of cell-matrix adhesions in 3D. We aim to study the mechanical interaction of these biological structures through a three dimensional discrete approach, reproducing the transmitting pattern force between the cytoskeleton and the extracellular matrix and how both parts are interplaying by them. This numerical model provides a discrete analysis of the proteins involved including spatial distribution, interaction between them, and study of the different phenomena, such as protein clutches unbinding or protein unfolding.

---

\*Corresponding author

*Email address:* [jmgaraz@unizar.es](mailto:jmgaraz@unizar.es) (J.M. García-Aznar)

*Keywords:* Actin, myosin, focal adhesion, 3D discrete model, extracellular matrix reorganization.

---

### **Highlights**

- A discrete computational model in 3D is proposed for reproducing the focal adhesion building phenomenon.
- The proposed model analyze the importance of the alignment between the matrix fiber and the cell protrusion on the size of the adhesion.
- The influence of different extracellular matrix properties on the size of the adhesion is also studied.

## 1. Introduction

Cell migration is crucial in a wide range of biological phenomena; during recent years great number of authors have put their effort to understand this process. It also plays a key role in many diseases like immune dysfunction or cancer development. It is a complex process, due to the high variability of morphology that cells show during migration and their strong dependency on environmental factors, such as dimensionality, stiffness of the matrix and chemical gradients [1].

In order to understand the mechanisms that regulate cell migration it is essential to study the interaction between the cell cytoskeleton and the extracellular matrix (ECM). This interaction is performed by a large multi-protein assembly that binds both parts forming the adhesion. These adhesions are commonly known as focal adhesions or focal contacts when they have matured, and nascent adhesions when they begin to form, which occurs in the cell edge in like-protrusion structures such as filopodia and lamellipodia [2]. This process of cell adhesion is the mechanism that ensures structural integrity of tissue [3], and it is mainly regulated by mechanical processes [4] [5].

During migration, myosin contractility and actin polymerization produce the forces responsible for the cyclic process of membrane protrusion and retrograde flow of F-actin at the leading edge [6, 7, 8]. These forces are transmitted to the ECM through trans-membrane receptors of the integrin family placed on the cell membrane [9], which serve as traction points over which the cell moves as well as sources of migration-related regulatory signals [1, 10, 11, 12]. These integrins are bound to the actin filaments in the cytoskeleton through a clutch of proteins that include talin,  $\alpha$ -actinin, vinculin and paxilin [13, 3, 14]. On the other side, integrins bind to protein ligands of the ECM, like fibronectin family [9]. Finally, the formed membrane protrusions must adhere to the matrix to define cell locomotion. If they do not attach, protrusions are unproductive and tend to move rearward in waves in response to the tension generated in the cell, in a process known as membrane ruffling [15]. Therefore, actin retrograde flow

is strongly dependent on cell contraction and focal adhesion size, concentration and strength [16].

Numerous studies over the past three decades have revealed a wealth of information detailing cell adhesion in two-dimensional surfaces. However, in  
35 *in-vivo* experiments many cells are completely surrounded by ECM which may have an influence on the size, composition and dynamics of adhesive structures. The study of cell adhesion in three-dimensional environments still remains in its infancy. This lack of knowledge together with the inherent computational cost of the corresponding simulations make these kind of 3D computational  
40 models a quite unexplored and challenging field. It is known that the way cells migrate changes between 2D and 3D environment [17]. Furthermore, in a 3D environment, cells of the same type migrate in different ways depending on the physical properties of the extracellular matrix, the degree of extracellular proteolysis and the soluble signaling factors [18] [19] [20]. Therefore, the key  
45 to develop more complex and reliable models to simulate cell migration in 3D environments lies on the incorporation of the elements that could clarify the mechanism of these migration changes.

Specific experiments in 3D environments were difficult to perform, but in the last two years these kind of studies have increased. Friedl and Wolf [21]  
50 analyzed how the ECM architecture along with some cellular determinants (such as concentration of some specific proteins) influence the different modes of cell migration in 3D environments. Haeger et al [22] studied what triggers the change on the invasion mode (single or collective) of mesenchymal tumor cells, observing that the ECM mechanical properties are the determining factor. Alessandri et  
55 al [23] studied how mechanical cues from the surrounding microenvironment may trigger cell invasion from a growing tumor. They used a revolutionary microfluidic technique that consists of the encapsulation and growth of cells inside permeable, elastic, hollow micro spheres. Another interesting study is the work by Kubow et al [24], where they identified the different mechanisms  
60 that determine adhesion in 3D matrices, observing cells growing along the ECM fibers.

Computational modeling is a useful tool for integrating the multiple subpro-  
cesses that govern cell motility and migration. In this field, Chan and Odde  
[25] investigated ECM rigidity sensing of filopodia via a stochastic model of the  
65 motor-clutch force transmission system in 2D. In their model, integrin molecules  
work as mechanical clutches linking F-actin to the substrate and mechanically  
resisting myosin-driven F-actin retrograde flow. More recently, Elosegui-Artola  
*et al.* [26] originally improved this model adjusting it for two different types  
of integrins and adding a reinforcement mechanosensing event which provokes  
70 an increment on the number of adhesions when the traction forces go over a  
threshold. Another interesting work is developed by Cirit *et al.* [27] where they  
created a model that analyzes the dynamical interplay between cell protrusion  
and adhesion at the cells leading edge. Milan *et al.* [28] developed a 3D model  
able to analyse the signals involved in cell adhesions in stem cells using the Cy-  
75 tokeleton Divided Medium model (CDM). The CDM model describes the cell  
like a set of particles interacting with each other and generating a discrete force  
network able to mimic the discrete filament network of the cytoskeleton in the  
cell. The model was also implemented to simulate how a cell adheres on plain  
substrate by emitting filopodia. With this cell model they were able to predict  
80 cytoskeleton reorganization and reinforcement during cell spreading.

*In vivo*, ECM consists of a myriad of fibers that are crosslinked between them  
forming a complex network which serves as a scaffold for the cells to migrate.  
When the cell adheres to the matrix and migrates, it moves along these fibers,  
deforming and reorienting them. Three aspects of the ECM are crucial for cell  
85 migration: mechanical properties, density and grade of fiber crosslinking. In  
this work, we assume that the local behavior of the ECM when a filopodium  
adheres to it does not depend on the global properties of the matrix. We also  
assume that the fiber is pre-stressed; therefore, we focus our study on the level  
of fiber crosslinking. The grade and strength of fiber crosslinkings determine the  
90 difficulty of the matrix to reorganize under cell forces. Alignment of the filopodia  
protrusion structures with the matrix fibers is necessary for the migration. If a  
protrusion adheres to a fiber and they are not aligned, the protrusion tries to

reorientate it in order to have more surface to adhere; if this is not possible, the protrusion cannot grow further and eventually disappears.

95 We present the simulation model detailing the equations and hypothesis in which it is based and how the model is implemented in a computer algorithm. The main goal of this model is to reproduce the adhesion degree between a cell filopodium (guided by non-muscle myosins) and a collagen fiber of the ECM depending on their relative orientations. Finally, we present how this model has  
100 been included in a computer algorithm.

## 2. Materials and Methods

Myosin force-generating process in the cytoskeleton provokes actin filaments dynamics. The forces are transmitted through an adhesion complex (AC) to the extracellular matrix. These adhesion complexes consist of a clutch of proteins  
105 that include cytoskeleton proteins (paxilin, talin, vinculin and so on) and transmembrane proteins called integrins. Extracellular matrix is deformed under these forces reorientating its fibers.

Due to the high variability of the studied phenomenon, the establishing of some simplifications and hypothesis is indispensable for the development of a  
110 model that simulates it. The computational cost and the complexity of a model that will include all the proteins involved in the phenomena would make the problem unapproachable.

Due to this, in this work, we have considered the effect of myosin proteins, only an actin filament, extracellular ligands, only a matrix fiber and adhesion  
115 complexes. Myosin exerts a force over a single actin filament causing its movement. This actin filament has been oversized in order to simulate a pack of filaments of a filopodium. The ACs bind to the actin monomers with the extracellular ligands that are distributed on the matrix fiber surface. They can be found in different scenarios: bound to actin and ligands, bound only to one of  
120 them and completely free. When they are bound to actin and ligand the adhesion grows and transmits the force. Although the ECM is a complex network

of fibers, Kubow et al [24] experimentally quantified that the adhesion size is mainly dependent on the alignment of one single fiber, giving support to our assumptions.

125 Therefore the simulation can be divided into three different parts: Actin-Myosin contractile complex, Adhesion complexes and ECM.

The present model is a 3D extension of a previous one, developed by the authors in the 2D case [29] but benefiting some improvements.

### 2.1. Actin-Myosin complex

130 The actin filament consists of a straight line of actin monomers, that only moves on the direction of its direction vector; therefore, only forces in this direction are considered. It is considered as a rigid solid under the assumption that the crosslinking matrix fibers stiffness is much lower than the union between monomers.

Myosins only exert pulling forces over the actin filament. The number of myosin heads bound to the actin filament determines the magnitude of the force. Each head is considered to produce a constant force of a fixed value. Thus, the total force is given by:

$$F_m = F_c \cdot n_m,$$

135 where  $F_c$  is the force exerted by each myosin head and  $n_m$  is the number of myosin heads attached to the filament. The ACs bound to the actin filament oppose to that force and, as a result of the balance of these two forces, the actin filament velocity can be obtained [25]:

$$v_{filament} = v_u \left(1 + \frac{F_r}{F_m}\right), \quad (1)$$

140 where  $F_r$  is the force applied by the bound ACs and  $v_u$  is the actin velocity for the unloaded filament, that is, when  $F_r = 0$ .

### 2.2. Adhesion Complexes (ACs)

The AC consists of a clutch of proteins with the function of binding the actin filament with the extracellular matrix. An AC is considered as two different

arms bound together, with the two free sides that bound to the actin monomers  
 145 or the ligands in the ECM. One arm is only able to bind to the actin and  
 the other only with the ligand. Both arms have the same model but different  
 mechanical properties, since one simulates the cytoskeleton proteins and the  
 other one simulates the integrin proteins.

Brownian dynamics regulate ACs behavior. In the next subsections are  
 150 detailed the equations that governs their behavior along with the different phe-  
 nomena proposed for them: binding-unbinding and folding-refolding.

### 2.2.1. Brownian Dynamics

We assume that the Langevin equation governs the dynamical behavior of  
 the ACs [30]. Therefore, if we consider the  $i$ -th AC,

$$m_i \frac{d^2 \mathbf{r}_i}{dt^2} = \mathbf{F}_i - \zeta_i \frac{d\mathbf{r}_i}{dt} + \mathbf{F}_i^B, \quad (2)$$

155 where  $m_i$  is the mass of the AC,  $r_i$  corresponds to its current position,  $\mathbf{F}_i$  are  
 the interaction forces among proteins,  $\zeta_i$  is the drag coefficient and  $\mathbf{F}_i^B$  is a  
 stochastic force. This equation allows the computation of the new position of  
 each particle for each time increment. In addition, considering that the inertial  
 effects of the ACs barely have an influence on the system in the considered time  
 160 scale, the acceleration term in equation (2) can be neglected, and therefore:

$$\frac{d\mathbf{r}_i}{dt} = \frac{1}{\zeta_i} (\mathbf{F}_i^B + \mathbf{F}_i). \quad (3)$$

In order to satisfy the fluctuation-dissipation theorem, the stochastic force,  $\mathbf{F}_i^B$ ,  
 is chosen from a random distribution verifying the following expectation values:

$$\langle \mathbf{F}_i^B(t) \rangle = 0, \quad \langle \mathbf{F}_i^B(t) \mathbf{F}_j^B(t) \rangle = \frac{2k_B T \zeta_i \delta_{ij}}{\Delta t} \boldsymbol{\delta}, \quad (4)$$

where  $k_B$  is the Boltzmann constant,  $T$  the absolute temperature,  $\delta_{ij}$  is the  
 165 Kronecker delta,  $\boldsymbol{\delta}$  the second order unit tensor and  $\Delta t$  the time increment con-  
 sidered in the simulation. As a first approach, it is considered for simplicity that



curve presents peak values around 30 pN, at 10nm intervals. Then, unfolding phenomena is regulated by the unfolding rate,  $k_{uf}$  [31]:

$$k_{uf} = \begin{cases} k_{uf}^0 \exp\left(\frac{\lambda_{uf} F_s}{k_B T}\right) & \text{if } r_{12} \geq r_0, \\ 0 & \text{if } r_{12} < r_0, \end{cases} \quad (7)$$

where  $\lambda_{uf}$  is the mechanical compliance,  $k_{uf}^0$  is the zero-force unfolding rate coefficient and  $F_s$  is the internal force of the AC seen in previous section, equation 185 (6).

When unfolding happens, it exists the possibility that the inverse phenomenon occurs, process known as refolding. This happens when the AC shrinks below the length at which the last unfolding occurred, then  $i^{th}$  unfolding 190 creases by 1.

Finally,  $k_{uf}$  corresponds to the rate parameter of an exponential distribution function, therefore the probability of the event is:

$$P = 1 - e^{-k_{uf} \Delta t}. \quad (8)$$

### 2.2.3. Binding/Unbinding

ACs present the possibility of separating from the actin filament or the 195 ligands when they are bound to them. This phenomenon is similar to the unfolding one, and it is governed by the unbinding rate,  $k_{ub}$  [31]:

$$k_{ub} = \begin{cases} k_{ub}^0 \exp\left(\frac{\lambda_{ub} F_s}{k_B T}\right) & \text{if } r_{12} \geq r_0, \\ 0 & \text{if } r_{12} < r_0, \end{cases} \quad (9)$$

where  $\lambda_{ub}$  is the mechanical compliance of the bond in the unbinding case and  $k_{ub}^0$  is the zero-force unbinding coefficient. In this model, when unbinding occurs, both arms of the AC refold completely and return to their resting state 200 ( $r_{12} = r_0$ ). The probability of this event is given by an exponential distribution function, similar to equation (8).

Free ACs can also bind to the actin filament or the ligands. This process is determined by the distance between them, occurring when.

$$d_{12} \leq 2^{1/6} \sigma_{12}, \quad (10)$$

$d_{12}$  being the distance between the two particles and  $\sigma_{12}$  the average diameter  
 205 of both particles.

It is important to remark that when an AC is bound only for one side (matrix fiber or actin filament), it is found in its equilibrium position. This equilibrium position corresponds to the radial direction of the matrix fiber or actin filament, respectively.

### 2.3. The Extracellular Matrix (ECM)

As it was described before, the ECM is a complex network of fibers which are crosslinked between them. The ECM is deformed and reorganized by cell-generated forces. As a first approach, we simulate a single matrix fiber which is considered as a rigid solid element with a spring on each of its ends to replicate the flexibility of the crosslinkers, simulating bending and torsional deformations in the fiber. Due to this, the possible movement and rotations of the fiber are given by the following expressions

$$F_{fib,i} = k_{fib,i} \mathbf{U}_{fib,i}, \quad M_{fib,i} = \tilde{k}_{fib,i} \theta_{fib,i},$$

where  $F_{fib,i}$  and  $M_{fib,i}$  are the force and torque vector, respectively;  $k_{fib,i}$  and  $\tilde{k}_{fib,i}$  are spring constants for displacement and torque, and  $U_{fib,i}$  and  $\theta_{fib,i}$  are the displacement and the rotation vectors for the matrix fiber, where the subindex  $i$  denotes the corresponding vector component.

215 We assume that the springs on the ends of the fiber have a similar behavior; so, we consider the same value for the corresponding constants  $k_{fib,i}$  and  $\tilde{k}_{fib,i}$ . The force vector is obtained from the forces exerted by the ACs attached to the ligands, and the torque vector is calculated by multiplying each discrete force by its distance to the fiber gravity center. Initially, as a first approach, we assume  
 220 a linear elastic behavior for the springs and  $k_{fib,i}$  and  $\tilde{k}_{fib,i}$  remain constant.

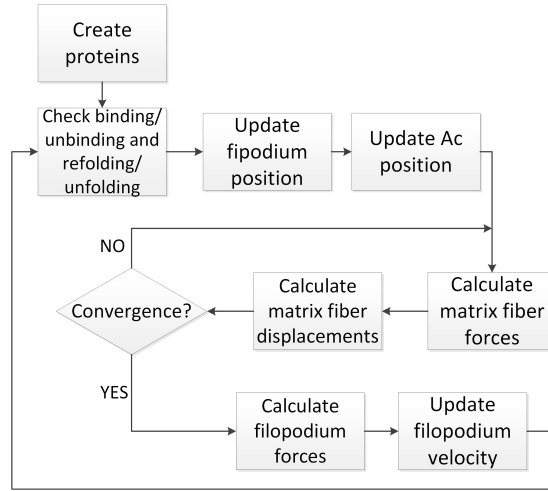


Figure 2: Flow chart of the implemented algorithm

#### 2.4. Numerical implementation

We have implemented a 3D computational model to reproduce the focal adhesion building phenomenon between a cell filopodium and an ECM fiber. Firstly, we set the initial conditions: The actin filament is a straight line of actin monomers with a fixed orientation. The matrix fiber is placed forming an initial angle  $\theta_0$  with the actin filament. The ligands can be placed randomly or with a uniform distribution on the matrix fiber surface. Finally the ACs are set randomly in the spatial domain of the simulation. Actin monomers and ligands are considered as spheres defined by their central point. ACs are defined by three points corresponding to two arms attached: the AC-actin point, that binds the AC with the actin monomers in the filament and corresponds to the edge of the actin-arm; the AC-matrix point, which corresponds to the edge of the matrix-arm and binds to ligands; and the AC-central point that corresponds to the point where both arms intersect.

The algorithm proposed for the spatio-temporal resolution of this problem is schematically shown in Fig. 2. It is solved in a discrete form, for each time increment,  $n$ . The algorithm is based on the following steps. First, given the initial conditions, an analysis of the current position of the ACs, actin monomers

and ligands is performed and the binding phenomenon is checked. Next, the  
240 actin filament moves, and as a consequence, the force balance in the system  
breaks the mechanical equilibrium. This provokes the deformation of the ACs  
bound for their both arms and consequently the increment of their tension.  
This tension provokes the matrix fiber displacement and rotation, requiring  
an iterative process to reach the force balance. When the ACs bound for their  
245 both arms are in balance, the unbinding and unfolding phenomena are analyzed.  
Finally, the new force on the actin filament is computed and therefore its velocity  
is obtained.

Fig. 3 shows the initial state of the simulation and the position of all the  
elements after 4 seconds of simulation. The whole video can be found in the  
250 supplementary material.

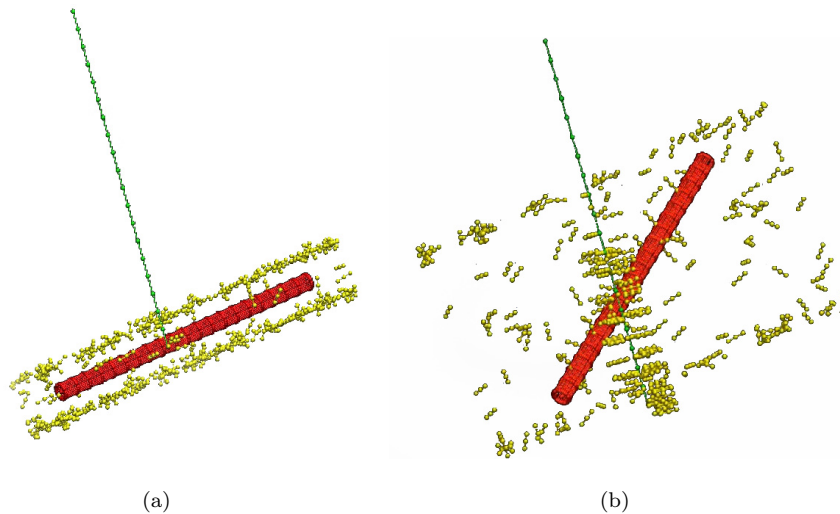


Figure 3: Representation of the different elements of the simulation (Actin: green ; ACs: yellow; Matrix fiber: red; Ligands: red points) at two different time steps: initial situation and after 4 seconds. At the beginning, there are no interactions and the matrix fiber remains at its resting state. After 4 seconds, the actin filament has moved over the matrix fiber, provoking the focal adhesion building and reorienting the fiber. (a) Initial state. (b) After 4 seconds of simulation

### 3. Results

We perform a first analysis of the studied phenomena, observing the influence of the relative orientation between the cell protrusion and the matrix fiber on the size of the adhesion. The local adhesion forming occurs during retrograde flow of actin filaments which is driven by myosin contraction. After, we study how some matrix and protein properties may also influence on the size of the adhesion. Since the model proposed present random properties, for all the results shown, we quantify the average of 20 simulations. The values of the parameters used in the model are shown in Table 1

#### 3.1. Local fiber alignment regulates adhesion size

The results of simulating an initial situation of 80 degrees between the actin filament and the matrix fiber are shown in Fig. 4. The adhesion size increases as the matrix fiber and the actin filament are more aligned. Qualitative interpretation of these results from the perspective of the model is straight forward: as the filament moves above the fiber, it starts to build adhesions; these adhesions begin to exert force on the matrix fiber provoking its movement (matrix reorganization) and a change on their relative position, increasing their alignment. This results in a closest position between the actin filament and the matrix fiber and the consequent increment on the number of adhesions.

#### 3.2. Effect of the fiber crosslinking stiffness and the initial orientation

We analyze the effect of four different matrix crosslinking rigidities (1000, 200, 50 and 5  $N/m$ ) on the adhesion size. We vary the initial orientation between the filopodium and the matrix fiber (80, 45 and 10 degrees) that will change along the simulations. We show the average of the adhesion size during each case. The results are shown in Fig. 5. We can observe that, in general, as the initial alignment increases the size of the adhesion grows bigger. When decreasing the stiffness, the size of the adhesion increases for 80 and 45 degrees of initial relative orientation since the more flexible the crosslinking is, the more fiber reorientation is permitted. However, when the initial relative orientation

Table 1: Numerical values for the model parameters.

Parameter	Symbol	Value	Source
Myosin head force	$F_c$	-2(pN)	[25]
Unloaded actin filament velocity	$v_u$	-120( $\mu\text{m/s}$ )	[25]
AC balance length	$r_0$	30 (nm)	estimated
AC arm length	$L_{AC}$	30 (nm)	estimated
Boltzman energy	$k_B T$	$4,142 \cdot 10^{-21}$ (J)	[30]
AC stiffness against compression below the equilibrium length	$k_{s,AC}$	0,004(N/m)	estimated
Zero-force unfolding rate coefficient	$k_{uf}^0$	$3 \cdot 10^{-5}(s^{-1})$	[31]
Mechanical compliance for the actin arm	$\lambda_{uf,actin}$	0,5 (nm)	estimated
Mechanical compliance for the matrix arm	$\lambda_{uf,matrix}$	0,5 (nm)	estimated
Zero-force unbinding rate coefficient	$k_{ub}^0$	$0,115(s^{-1})$	[31]
Mechanical compliance of the actin bond for unbinding	$\lambda_{ub,actin}$	0,5 (nm)	estimated
Mechanical compliance of the matrix bond for unbinding	$\lambda_{ub,matrix}$	0,5 (nm)	estimated
Persistence length for the actin arm	$p_{actin}$	0,04 (nm)	estimated
Persistence length for the matrix arm	$p_{matrix}$	0,04 (nm)	estimated
Maximum number of unfolding for both arms	$n_{uf}$	2	estimated
Simulation step time	$\Delta t$	0,005 (s)	estimated
Total time of the simulation	t	10 (s)	estimated
Actin monomer diameter	$\sigma_A$	70 (nm)	estimated
Ligand diameter	$\sigma_L$	7 (nm)	estimated
Medium viscosity for the AC arms	$\eta$	$8,599 \cdot 10^{-4}$ (kg/m s)	[30]
Fiber crosslinking stiffness to translation [x,y,z]	$k_{fib,i}$	[5, 5, 5]N/m	estimated
Fiber crosslinking stiffness to rotation [x,y,z]	$\tilde{k}_{fib,i}$	[5, 5, 5](nN · nm/rad)	estimated
Fiber length	$L_{fib}$	5000 nm	estimated

280 is 10 degrees, this behavior is not observed. In this case, the fiber and actin filament are almost fully aligned; therefore, the reorganization of the matrix fiber is not needed and the adhesion size mainly depends on the stochastic of binding and unbinding phenomena. This behavior can be seen clearly in Fig.

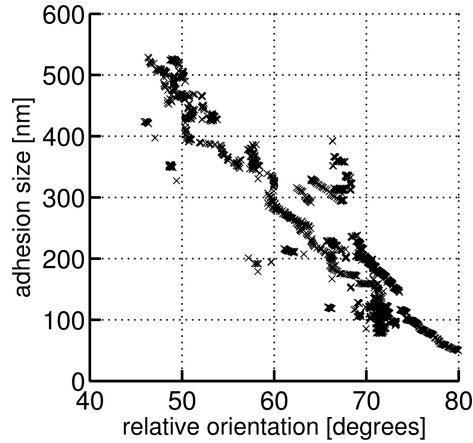


Figure 4: Adhesion size depending on the level of alignment between the actin filament and the matrix fiber. The initial angle between them is 80 degrees. As the adhesion starts to build, the fiber is reorientated by the cell forces, increasing in this way their alignment (the relative angle between them decreases), which also makes the adhesion bigger.

Table 2: Reference values and range of variation of the values for the sensitivity analysis of the initial conditions.

Parameter	Ref. value	Sensitivity analysis
Matrix fiber radio ( $r_{fib}$ )	300nm	150nm
Ligands concentration	$1.5 \cdot 10^{-3} (ligands/nm^2)$	$(1.2 - 0.9 - 0.6) \cdot 10^{-3} ligands/(nm^2)$
Initial orientation	80	10 - 45
Fiber crosslinking stiffness, translation and rotation [x,y,z]	$[5, 5, 5](N/m) - (nN \cdot nm/rad)$	$[5, 5, 5] \cdot 10 - [2, 2, 2] \cdot 10^2 - [1, 1, 1] \cdot 10^3(N/m) - (nN \cdot nm/rad)$
Mechanical compliance for actin and matrix arm	$[0.5, 0.5](nm)$	$[0, 0.5]-[0.5, 0] (nm)$

285 6, where the relation between adhesion size and fiber alignment is shown. We can observe that, for this case, proportionality between alignment and adhesion size shown in the first case is lost.

### 3.3. Effect of matrix fiber diameter

290 The focal adhesion building phenomenon is strongly influenced by the geometrical properties of the ECM. The diameter of the matrix fibers is one of the most important factor to consider, since it regulates the geometrical lim-

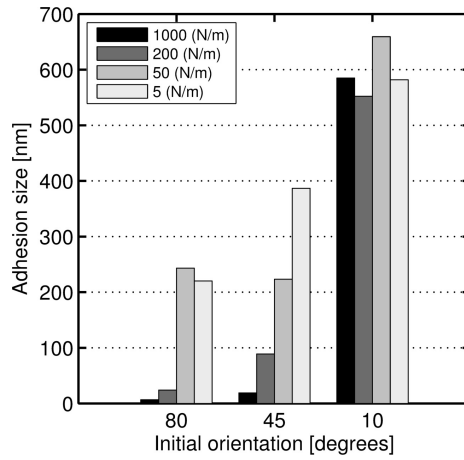


Figure 5: Average of the adhesion size, for 10 seconds of simulation, depending on the initial orientation between actin filament and matrix fiber, considering different fiber crosslinking stiffness. For initial angles of 80 and 45 degrees, increasing the stiffness has a negative impact on the adhesion size. When the initial orientation is 10 degrees, the adhesion size is not affected by fiber crosslinking stiffness since they already are almost fully aligned.

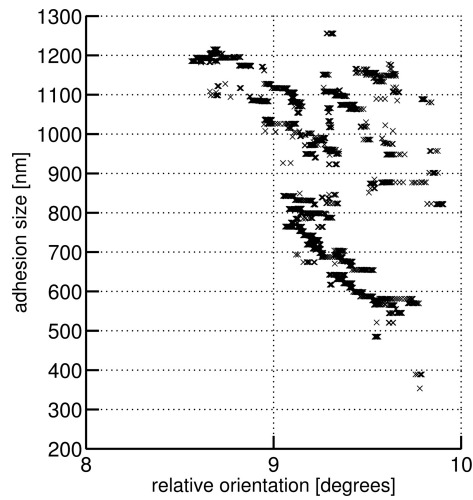


Figure 6: Adhesion size against level of relative orientation between matrix fiber and actin filament. The initial value for the orientation is 10 degrees. Fiber orientation barely changes and it is not determinant on the adhesion size.

its for the adhesion. In Fig. 7, we show the same case of section 3.2 with a reduced diameter. The results show that when the crosslinking fibers present

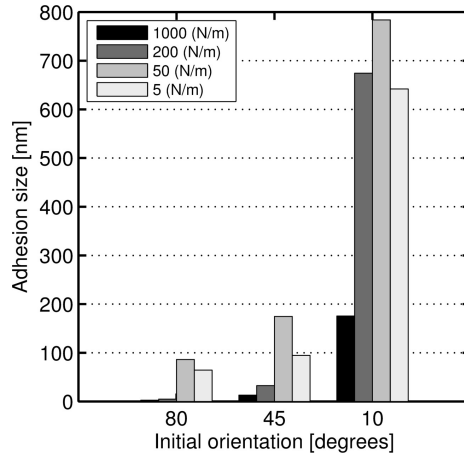


Figure 7: Sensitivity analysis of the fiber diameter (diameter= 150nm). The adhesion size depends on the initial level of alignment for different fiber crosslinking stiffness and different initial grade of alignment. In general, as the fiber diameter increases, more surface the cell protrusion has to bind to; therefore, the adhesion size increases. This fact loose importance when the fiber is initially aligned, or when the fiber crosslinkers are very soft, since the cell filopodium quickly alines to the fiber. For these cases, the adhesion occurs along the length of the fiber, resting importance to its diameter size.

more stiffness the matrix fiber thickness clearly influence the adhesion size.

### 3.4. Effect of the ligand concentration

295 The ligand concentration is a determining regulator of cell matrix adhe-  
sions. This variable, relatively easy to change experimentally, has a huge im-  
pact on this phenomenon. To analyze its effect on the proposed model we have  
carried out numerical simulations with four different concentration of ligands:  
 $1.5 \cdot 10^{-3}$ ,  $1.2 \cdot 10^{-3}$ ,  $0.9 \cdot 10^{-3}$  and  $0.6 \cdot 10^{-3} \text{ligand}/(\text{nm}^2)$ . These concentration  
300 values correspond to the reference value and to its 80%, 60% and 40% value,  
respectively. The obtained results are shown in Fig. 8. When reducing the lig-  
and concentration, the adhesion size also decreases. Ligands serve as anchoring  
points for the ACs, therefore a depletion in their number difficults the formation  
of adhesions.

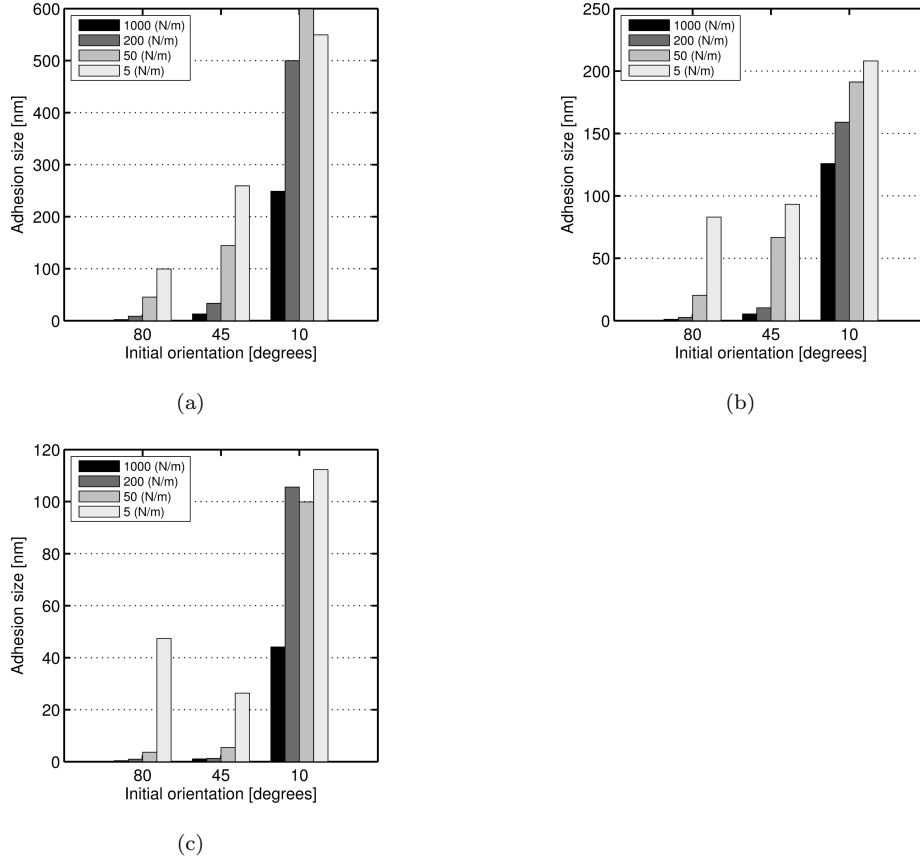


Figure 8: Sensitivity analysis of ligand concentration. In each graph it is shown the adhesion size depending on the initial level of alignment for different fiber crosslinking stiffness. By reducing the ligand concentration, smaller adhesions are obtained, since it is more difficult for the ACs to bind. (a)  $1.2 \cdot 10^{-3} \text{ ligands}/(\text{nm}^2)$  (b)  $0.9 \cdot 10^{-3} \text{ ligands}/(\text{nm}^2)$  (c)  $0.6 \cdot 10^{-3} \text{ ligands}/(\text{nm}^2)$ .

305 **3.5. Effect of the unbinding rate**

In the model, ACs bound to both sides can unbind from actin filament or from ligands on the matrix fiber. However, phenomenologically it is not clear whether it unbinds more from one side or another. In order to address this question, we have conducted some tests forbidding the unbinding in one side  
 310 and maintaining it on the other side. The considered parameters are the given in Section 3.2. The obtained results are shown in Fig. 9. We can observe that,

when the ACs only separate from the actin filament, the adhesion size is larger than when the AC only unbinds from the ligands on the matrix fiber. This results can be explained from a geometric point of view: finding the actin filament is easier than finding a free ligand to bind since the actin filament is considerably bigger; therefore, when an AC separates from a ligand on the matrix fiber, it is more difficult for the AC to bind again, which ultimately provokes a smaller adhesion. In addition, we can see that in both cases the adhesion size is higher than in the case when unbinding phenomenon is permitted from both sides, since in the latter case, the adhesion has higher possibilities of breaking.

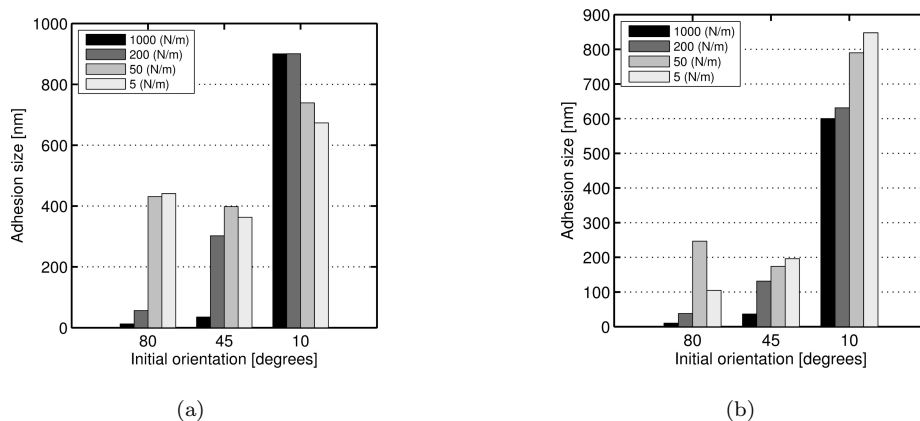


Figure 9: Different unbinding places. In each graph the adhesion size average depending on the initial alignment between actin filament and matrix fiber for different fiber crosslinking stiffness is shown. Since the actin filament is bigger and easier to find than a free ligand, when the ACs only separate from the actin filament, the adhesion size is larger than the adhesion when the AC only unbinds from the ligands on the matrix fiber. (a) Only unbinding from actin is permitted (b) Only unbinding from ligand is permitted.

#### 4. Discussion

Computational works in biology help us to unravel fundamental mechanisms that can be observed in experiments, but that require further analysis for a better understanding. Here, we have presented a discrete numerical study providing an individual insight of the role that different components play on the

cell-matrix adhesions, in particular, it reproduces the building of local adhesions between a filopodium and a single matrix fiber during actin retrograde flow.

To our knowledge, this model for cell-matrix adhesions in a 3D environment, considering a matrix-fiber approach, is novel and original. We have observed  
330 that the alignment between the myosin retraction and the matrix fiber is crucial for the maturation of the focal adhesions and therefore essential for cell migration. Due to this, it is worth to analyze how different conditions or scenarios may regulate this process. In this case, we have considered that ACs are flexible elements with a non-linear behavior and they present some important properties, such as binding-unbinding or unfolding-refolding. We have also considered  
335 the spatial distribution of the ligands on the ECM, that determines the pattern of how the traction forces are transmitted to the matrix fiber. This model offers the possibility of analyzing, individually, the influence of the different proteins involved in the mechano-biological process: the ligand concentration determining the adhesion size or the impact of the initial orientation between  
340 the filopodium and the matrix fiber. In addition, we also consider how the matrix fiber crosslinking stiffness influence the capacity of the ECM to reorganize under cell-generated forces.

Qualitatively, the tendency obtained between the relative orientation of the  
345 filopodia and the matrix fibers was already confirmed experimentally by different authors [24]. Moreover, Kubow et al [24] showed that the local fiber size also has a significant role in 3D adhesions, in such a way that the adhesive area in the fiber depends not only on the fiber orientation, but also in the fiber size. The model proposed here is also consistent with those experimental observations, as  
350 shown in the analysis of the matrix fiber diameter. Furthermore, this model also allows us to study a wide range of conditions providing a lot of information of how local properties of both matrix and cell regulate this process, becoming a powerful tool that provides an interesting insight of how the phenomenon responds under those conditions.

355 The formulation of some hypothesis and simplifications is a crucial and indispensable part when building a model. It is essential that they should be

selected accordingly with the biology of the phenomenon. In this work, we have assumed that locally, the property of one matrix fiber is more determining than the whole ECM properties. In addition, we have set the hypothesis that the fiber is pre-stressed and that the cell forces are not able to deform it, assuming  
360 that the fiber deformability is mainly due to the deformation of the crosslinkers that links the different fibers. Moreover, referring to the fiber crosslinkers, we have assumed as a first approach that they have a linear behavior and they cannot break.

*In vivo*, ECM fibers are usually loose and they tighten and deform when  
365 cells exert forces over them, in fact, until they are not tight, cells are not able to move along them. For example, collagen type I exhibits a viscoelastic behavior, they store elastic energy and partially relax internal stress through dissipative process [33]. The fiber crosslinkers exhibit a complex behavior and when they  
370 are subjected to a high level of force they can break down. Despite all these differences, the proposed model reproduces reliably the addressed phenomenon. In the same ECM, at a local level, properties can change within a certain range depending on the zone. With the proposed hypothesis, and based on the experimental data observed in literature, we have shown that the size of the adhesion  
375 (depending on the relative orientation between protrusion and matrix fiber) presents a real behavior pattern that fits in that range.

Crucial phenomena in cell migration process are addressed in this work. The relevant process of how cells exert forces over the ECM, provoking its reorganization, is studied. The role of matrix fiber stiffness in this process is analyzed  
380 through numerical simulations, observing that the stiffer the crosslinkings are, the more difficult to reorganize the ECM by the cell is. A tendency to always try to obtain the largest adhesion size is remarked. This helps the cells to regulate their migration. To conclude, the discrete modeling presented here is a relevant tool to improve the understanding of cell matrix-adhesions and to go deeper on  
385 the biological knowledge of these processes.

The next step for this model is to include more matrix fibers and simulate how a cell would adhere to them. This improvement would offer the possi-

bility of analyzing how matrix micro architecture influence on cell movement. Cells, during migration, may find very different matrix architectures at different points, exhibiting consequently different behaviors. Analyzing the role of  
390 different parameters that define the matrix architecture (fiber density and orientation, pore confinement and connectivity) is a promising path to follow in order to understand 3D cell migration.

### Acknowledgments

395 This study is supported by the European Research Council (ERC) through project ERC-2012-StG 306751 and the Spanish Ministry of Economy and Competitiveness (DPI2012-38090-C03-01).

### References

- [1] J. T. Parsons, A. R. Horwitz, M. a. Schwartz, Cell adhesion: integrating  
400 cytoskeletal dynamics and cellular tension., *Nature reviews. Molecular cell biology* 11 (9) (2010) 633–43. doi:10.1038/nrm2957.
- [2] B. Geiger, A. Bershadsky, R. Pankov, K. M. Yamada, B. G. Correspondence, Transmembrane extracellular matrix-cytoskeleton crosstalk, *Nature Reviews —Molecular Cell Biology* 2 (November) (2001) 793–805.
- 405 [3] C. Selhuber-Unkel, T. Erdmann, M. López-García, H. Kessler, U. S. Schwarz, J. P. Spatz, Cell adhesion strength is controlled by intermolecular spacing of adhesion receptors., *Biophysical journal* 98 (4) (2010) 543–51. doi:10.1016/j.bpj.2009.11.001.
- [4] D. E. Discher, P. Janmey, Y.-L. Wang, Tissue cells feel and respond to the  
410 stiffness of their substrate., *Science (New York, N.Y.)* 310 (5751) (2005) 1139–43. doi:10.1126/science.1116995.
- [5] V. Vogel, M. Sheetz, Local force and geometry sensing regulate cell functions., *Nature reviews. Molecular cell biology* 7 (4) (2006) 265–75. doi:10.1038/nrm1890.

- 415 [6] A. Ponti, M. Machacek, S. L. Gupton, C. M. Waterman-Storer,  
G. Danuser, Two distinct actin networks drive the protrusion of mi-  
grating cells., *Science (New York, N.Y.)* 305 (5691) (2004) 1782–6.  
doi:10.1126/science.1100533.
- [7] T. D. Pollard, G. G. Borisy, Cellular motility driven by assembly and dis-  
420 assembly of actin filaments., *Cell* 112 (4) (2003) 453–65.
- [8] B. Sabass, U. S. Schwarz, Modeling cytoskeletal flow over adhesion sites:  
competition between stochastic bond dynamics and intracellular relax-  
ation., *Journal of physics. Condensed matter : an Institute of Physics*  
*journal* 22 (19) (2010) 194112.
- 425 [9] E. Ruoslahti, RGD and other recognition sequences for integrins., *An-  
nual review of cell and developmental biology* 12 (1996) 697–715.  
doi:10.1146/annurev.cellbio.12.1.697.
- [10] A. J. Ridley, M. a. Schwartz, K. Burridge, R. a. Firtel, M. H. Ginsberg,  
G. Borisy, J. T. Parsons, A. R. Horwitz, Cell migration: integrating signals  
430 from front to back., *Science (New York, N.Y.)* 302 (5651) (2003) 1704–9.  
doi:10.1126/science.1092053.
- [11] L. Chen, M. Vicente-Manzanares, L. Potvin-Trottier, P. W. Wiseman, A. R.  
Horwitz, The integrin-ligand interaction regulates adhesion and migration  
through a molecular clutch., *PloS one* 7 (7) (2012) e40202.
- 435 [12] R. F. Loeser, Integrins and chondrocyte-matrix interactions in articular  
cartilage., *Matrix biology : journal of the International Society for Matrix*  
*Biology* 39 (2014) 11–16. doi:10.1016/j.matbio.2014.08.007.
- [13] E. Zamir, B. Geiger, Molecular complexity and dynamics of cell-matrix  
adhesions., *Journal of cell science* 114 (Pt 20) (2001) 3583–90.
- 440 [14] C. a. Abbey, K. J. Bayless, Matrix density alters zyxin phosphoryla-  
tion, which limits peripheral process formation and extension in en-

- dothelial cells invading 3D collagen matrices., *Matrix biology : journal of the International Society for Matrix Biology* 38 (2014) 36–47. doi:10.1016/j.matbio.2014.06.006.
- 445 [15] B. Borm, R. P. Requardt, V. Herzog, G. Kirfel, Membrane ruffles in cell migration: indicators of inefficient lamellipodia adhesion and compartments of actin filament reorganization., *Experimental cell research* 302 (1) (2005) 83–95. doi:10.1016/j.yexcr.2004.08.034.
- [16] D.-H. Kim, D. Wirtz, Focal adhesion size uniquely predicts cell migration., *FASEB journal : official publication of the Federation of American Societies for Experimental Biology* 27 (4) (2013) 1351–61. 450 doi:10.1096/fj.12-220160.
- [17] J. S. Harunaga, K. M. Yamada, Cell-matrix adhesions in 3D., *Matrix biology : journal of the International Society for Matrix Biology* 30 (7-8) 455 (2011) 363–8. doi:10.1016/j.matbio.2011.06.001.
- [18] R. J. Petrie, K. M. Yamada, At the leading edge of three-dimensional cell migration., *Journal of cell science* 125 (Pt 24) (2012) 5917–26. doi:10.1242/jcs.093732.
- [19] V. Sanz-Moreno, C. Gaggioli, M. Yeo, J. Albregues, F. Wallberg, A. Viros, S. Hooper, R. Mitter, C. C. Féral, M. Cook, J. Larkin, R. Marais, 460 G. Meneguzzi, E. Sahai, C. J. Marshall, ROCK and JAK1 signaling cooperate to control actomyosin contractility in tumor cells and stroma., *Cancer cell* 20 (2) (2011) 229–45. doi:10.1016/j.ccr.2011.06.018.
- [20] K. Wolf, I. Mazo, H. Leung, K. Engelke, U. H. von Andrian, E. I. Deryugina, A. Y. Strongin, E.-B. Bröcker, P. Friedl, Compensation mechanism in 465 tumor cell migration: mesenchymal-amoeboid transition after blocking of pericellular proteolysis., *The Journal of cell biology* 160 (2) (2003) 267–77. doi:10.1083/jcb.200209006.

- 470 [21] P. Friedl, K. Wolf, Plasticity of cell migration: a multiscale tuning model., *The Journal of cell biology* 188 (1) (2010) 11–9. doi:10.1083/jcb.200909003.
- [22] A. Haeger, M. Krause, K. Wolf, P. Friedl, Cell jamming: Collective invasion of mesenchymal tumor cells imposed by tissue confinement., *Biochimica et biophysica acta* doi:10.1016/j.bbagen.2014.03.020.
- 475 [23] K. Alessandri, B. R. Sarangi, V. V. Gurchenkov, B. Sinha, T. R. Kießling, L. Fetler, F. Rico, S. Scheuring, C. Lamaze, A. Simon, S. Geraldo, D. Vignjevic, H. Doméjean, L. Rolland, A. Funfak, J. Bibette, N. Bremond, P. Nassoy, Cellular capsules as a tool for multicellular spheroid production and for investigating the mechanics of tumor progression in vitro., *Proceedings of the National Academy of Sciences of the United States of America* 480 110 (37) (2013) 14843–8. doi:10.1073/pnas.1309482110.
- [24] K. E. Kubow, S. K. Conrad, a. R. Horwitz, Matrix microarchitecture and myosin II determine adhesion in 3D matrices., *Current biology : CB* 23 (17) (2013) 1607–19. doi:10.1016/j.cub.2013.06.053.
- 485 [25] C. E. Chan, D. J. Odde, Traction Dynamics of Filopodia on Compliant Substrates, *Science (New York, N.Y.)* 322 (December) (2008) 1687–1691.
- [26] A. Elosegui-Artola, E. Bazellères, M. D. Allen, I. Andreu, R. Oria, R. Sunyer, J. J. Gomm, J. F. Marshall, J. L. Jones, X. Trepate, P. Roca-Cusachs, Rigidity sensing and adaptation through regulation of integrin types., *Nature materials* 13 (6) (2014) 631–7. doi:10.1038/nmat3960. 490
- [27] M. Cirit, M. Krajcovic, C. K. Choi, E. S. Welf, A. F. Horwitz, J. M. Haugh, Stochastic model of integrin-mediated signaling and adhesion dynamics at the leading edges of migrating cells., *PLoS computational biology* 6 (2) (2010) e1000688. doi:10.1371/journal.pcbi.1000688.
- 495 [28] J.-l. Milan, S. Lavenus, P. Pilet, G. Louarn, S. Wendling, D. Heymann, P. Layrolle, P. Chabrand, Computational model combined with in vitro

experiments to analyse mechanotransduction during mesenchymal stem cell adhesion., *European Cells and Materials* 25 (2013) 97–113.

- [29] J. Escribano, M. T. Sánchez, J. M. García-Aznar, A discrete approach  
500 for modeling cellmatrix adhesions, *Computational Particle Mechanics* 1 (2)  
(2014) 117–130. doi:10.1007/s40571-014-0006-7.
- [30] T. Kim, W. Hwang, R. D. Kamm, Computational Analysis of a Cross-  
linked Actin-like Network, *Experimental Mechanics* 49 (1) (2007) 91–104.
- [31] T. Kim, W. Hwang, R. D. Kamm, Dynamic role of cross-linking pro-  
505 teins in actin rheology., *Biophysical journal* 101 (7) (2011) 1597–603.  
doi:10.1016/j.bpj.2011.08.033.
- [32] G. Bao, Mechanics of biomolecules, *Journal of the Mechanics and Physics  
of Solids* 50 (11) (2002) 2237–2274.
- [33] S. Münster, L. M. Jawerth, B. a. Leslie, J. I. Weitz, B. Fabry, D. a.  
510 Weitz, Strain history dependence of the nonlinear stress response of fib-  
rin and collagen networks., *Proceedings of the National Academy of  
Sciences of the United States of America* 110 (30) (2013) 12197–202.  
doi:10.1073/pnas.1222787110.